Functional Characterization of Adrenocortical Masses in Nononcologic Patients Using ^{68}Ga-Pentixafor

Jie Ding[1], Anli Tong[2], Yushi Zhang[3], Jin Wen[3], Hui Zhang[4], Marcus Hacker[5], Li Huo[1], and Xiang Li[5]

[1]Department of Nuclear Medicine, Beijing Key Laboratory of Molecular Targeted Diagnosis and Therapy in Nuclear Medicine and State Key Laboratory of Complex Severe and Rare Diseases, Peking Union Medical College Hospital, Chinese Academy of Medical Science and Peking Union Medical College, Beijing, China; [2]Department of Endocrinology and Key Laboratory of Endocrinology, Ministry of Health, Peking Union Medical College Hospital, Chinese Academy of Medical Science and Peking Union Medical College, Beijing, China; [3]Department of Urological Surgery, Peking Union Medical College Hospital, Chinese Academy of Medical Science and Peking Union Medical College, Beijing, China; [4]Department of Pathology, Peking Union Medical College Hospital, Chinese Academy of Medical Science and Peking Union Medical College, Beijing, China; and [5]Division of Nuclear Medicine, Department of Biomedical Imaging and Image-Guided Therapy, Medical University of Vienna, Vienna, Austria

We aimed to investigate the diagnostic and prognostic value of ^{68}Ga-pentixafor PET/CT imaging in noncancer patients with suspected adrenal masses. **Methods:** Sixty-four patients who had benign adrenal masses on CT were retrospectively included in our study. All patients underwent ^{68}Ga-pentixafor PET/CT, and 56 of these patients subsequently underwent adrenalectomy. The subtypes of 81 adrenal tumors, including 14 nonfunctioning adrenal nodules, 4 cortisol-producing adenomas, 41 aldosterone-producing adenomas, 5 cases of suspected unilateral adrenal hyperplasia, 15 cases of idiopathic aldosterone hyperplasia, and 2 pheochromocytomas, were determined by histology or follow-up evaluations. The diagnostic efficiency of functional lateralization was calculated by visual analysis. Semiquantitative parameters of these lesions, including SUV_{max}, the ratio of lesional SUV_{max} to normal liver SUV_{mean} (LLR), and the ratio of lesional SUV_{max} to contralateral adrenal tissue SUV_{mean} (LCR), were also calculated. Dynamic analysis was also performed on 15 patients. In addition, clinical outcomes were assessed and compared in patients who underwent adrenalectomy. **Results:** The sensitivity and specificity of ^{68}Ga-pentixafor PET for functional lateralization in patients with adrenocortical lesions were 97.8% (45/46) and 87.5% (14/16), respectively. The 2 pheochromocytoma lesions had lower pentixafor uptake than the normal adrenal glands. Functioning (active) adrenocortical adenomas showed an elevated SUV_{max} of 16.3 ± 7.9, in comparison to 4.4 ± 1.7 in nonfunctioning (inactive) adenomas and 5.5 ± 2.7 in hyperplasia lesions ($P < 0.0001$). To identify active adrenocortical adenomas, a cutoff of 7.1 for SUV_{max} showed a sensitivity of 90.9% and a specificity of 85.3% (area under receiver-operating-characteristic curve, 0.96; $P < 0.0001$); a cutoff of 2.5 for LLR showed a sensitivity of 95.5% and a specificity of 88.2% (area under receiver-operating-characteristic curve, 0.97; $P < 0.0001$); and a cutoff of 2.4 for LCR showed a sensitivity of 88.6% and a specificity of 91.8% (area under receiver-operating-characteristic curve, 0.95; $P < 0.0001$). The graphical influx rate constant of active adrenocortical adenomas was significantly higher than that of inactive adenomas. Uptake values for ^{68}Ga-pentixafor were significantly higher in patients with preferable outcomes (cured/improved) (SUV_{max}, 15.5 ± 8.0; LLR, 6.5 ± 4.3; LCR, 6.2 ± 5.0) than in patients with nonpreferable outcomes (no improvement) (SUV_{max}, 4.2 ± 0.5; LLR, 1.3 ± 0.2; LCR, 1.5 ± 0.6; all $P < 0.0001$). **Conclusion:** ^{68}Ga-pentixafor PET/CT imaging exhibits great potential for noninvasive functional lateralization and characterization in patients with adrenocortical masses.

Key Words: adrenocortical masses; endocrine hypertension; ^{68}Ga-pentixafor

The widespread use of conventional imaging modalities has increased the identification of adrenal masses. Adrenocortical adenomas, which are generally nonfunctioning adrenal adenomas (NFAs), account for 36%–94% of adrenal incidentalomas diagnosed in patients without malignant diseases (1). As compared with NFAs, functional adrenocortical adenomas are associated with increased morbidity and elevated mortality. Adrenalectomy is indicated in patients with suspected malignancies or functional adrenal tumors, whereas active surveillance is recommended for patients with NFAs (2).

Thereby, it is essential to determine the hormonal secretion of adrenal lesions (e.g., aldosterone-producing adenoma [APA] causing primary hyperaldosteronism [PA], cortisol-producing adenoma [CPA] in Cushing syndrome patients, or pheochromocytomas vs. NFAs), and lateralizing the disease to a single adrenal gland (e.g., unilateral APA or unilateral adrenal hyperplasia [UAH] vs. idiopathic aldosterone hyperplasia [IAH] in PA patients or unilateral vs. bilateral functional adenoma) is essential for surgical management for adrenal benign lesions; bilateral IAHs are treated with medication (2–4).

Identifying the functional distinctions between adrenal nodules remains challenging (3,4). The functional diagnostic workup of adrenal masses, including screening, confirmatory tests, and subtype differentiation, is based on a combination of clinical symptoms, the presence of adrenal hormonal disorders, radiographic features, and the results of adrenal venous sampling (AVS). AVS is highly recommended for lateralization because of the increased occurrence rate of NFA in older patients (>35 y old) (4,5). However, the clinical manifestations of endocrine diseases are diverse, and a lack of uniformity in diagnostic protocols and assay methods for determining hormonal disorders in adrenal masses results in significant variability in measurements. Besides, conventional

imaging provides lesional morphology but not its functional status. If the diagnosis is based solely on adrenal CT, nonfunctional unilateral adrenal macroadenomas are indistinguishable from APAs, and small APAs may be misidentified as IAH by radiologists (3). An effective and noninvasive workup would be helpful to obviate AVS for the characterization of adrenal masses and their therapeutic management.

The potential utility of molecular imaging in the investigation of adrenal disorders has been recognized. The CXC chemokine receptor type 4 (CXCR4), which is a G protein–coupled receptor expressed on the surface of the cell membrane, contributes to the development and progression of malignancies. CXCR4 expression has been reported to be upregulated in APAs and CPAs; however, its expression is almost negligible in NFAs (6). Besides, CXCR4 is also hardly expressed by the tumor cells in paragangliomas (7). ^{68}Ga-pentixafor, a CXCR4-specific PET tracer, may therefore be effective for the evaluation of the functional lateralization of adrenal lesions and identification of functional adrenocortical adenomas. In this pilot study, we aimed to develop ^{68}Ga-pentixafor PET/CT as a noninvasive test for the recognition of functional adrenocortical lesions and to help guide the management of nononcologic patients with suspected adrenal tumors.

MATERIALS AND METHODS

Patients and Clinical Diagnosis

In this retrospective study, we included 66 nononcologic patients with adrenal nodules who underwent ^{68}Ga-pentixafor PET/CT examinations between August 1, 2018, and August 30, 2019. The patients with a history of malignancy were excluded. Before PET/CT examination, adrenal CT was performed. A series of continuous patients with adrenal disease who had features of benign adrenal masses (homogeneous lesions with smooth margins) identified on adrenal CT were included in our study. The patients were referred to us by a certified specialist in clinical endocrinology or in urology, because the adrenal masses were incidentally ($n = 55$) or specifically (e.g., patients with endocrine symptoms, $n = 11$) discovered during an abdominal imaging procedure.

Two patients with a malignant adrenal lesion or a nonadrenal lesion were excluded. Thus, 64 patients were analyzed in this study, with diagnoses based on clinical variables, laboratory assessment, adrenal CT imaging, AVS examination (4 patients), histopathologic examination, and follow-up evaluation (median, 22.5 ± 4.1 mo). The diagnostic criteria are listed in the supplemental materials, which are available at http://jnm.snmjournals.org (8,9).

Written informed consent to undergo ^{68}Ga-pentixafor PET imaging was obtained from all patients, and the consent form and study were approved by the Ethical Committee of Peking Union Medical College Hospital (institutional review board protocol ZS-1435).

Static and Dynamic PET Imaging

The ^{68}Ga-pentixafor was prepared as previously described (10), with a radiochemical purity of at least 95%. All images were acquired using a dedicated PET/CT scanner (PoleStar m660; SinoUnion Health Care Inc.) at the Peking Union Medical College Hospital. Fifteen patients with 16 adrenal lesions (including 11 APA lesions and 5 NFA lesions) underwent 30-min dynamic imaging starting immediately after intravenous injection of a ^{68}Ga-pentixafor bolus (128.0 ± 77.0 MBq). The reconstruction methods are described in the supplemental materials. In the other 49 patients, static imaging of the upper abdomen and adrenal region was performed over 5 min using a single bed position, with an uptake time of 25–30 min after injection of 87.7 ± 64.8 MBq of ^{68}Ga-pentixafor.

Imaging Analysis

On visual analysis of the static images, ^{68}Ga-pentixafor–avid adrenal nodules were defined as those showing a higher uptake of ^{68}Ga-pentixafor on PET imaging than was present in the ipsilateral or contralateral normal adrenal glands. The scan was considered negative if it showed ^{68}Ga-pentixafor uptake equal to or less than that in the normal adrenal glands. The presence of ^{68}Ga-pentixafor–avid adrenal nodules indicated the adrenal lateralization.

For semiquantitative analysis of ^{68}Ga-pentixafor PET/CT data, spheric volumes of interest were assigned to the center of adrenal lesions using CT images and the normal adrenal gland. Another volume of interest was placed in the liver adjacent to the right adrenal gland (2-cm-diameter sphere). The SUV_{max} of lesions, the ratio of the lesional SUV_{max} to the normal liver SUV_{mean} (LLR), and the ratio of the lesional SUV_{max} to the contralateral adrenal tissue SUV_{mean} (LCR) were calculated.

All scans were interpreted by nuclear medicine physicians experienced in ^{68}Ga-pentixafor PET; they were unaware of the clinical information. A joint reevaluation was performed if the interpretation was incongruent. The preliminary results that were categorized as lateralization (e.g., negative or positive on the right, on the left, on bilaterally) were used to assist the clinician in the diagnosis and management of patients. On completion of the follow-up, all scans were retrospectively reviewed. The results that represented a clinical diagnosis with lateralization (e.g., APA, left, or CPA, right) were used for the final retrospective analysis (Supplemental Table1).

Patient Therapy Management and Outcomes

The management of patients was codetermined by endocrinologists and urologists on the basis of the clinical and imaging presentations. Fifty-six patients underwent adrenalectomy with subsequent pathologic analysis. Of these, 47 patients (83.9%) underwent adrenalectomy for suspected adrenal endocrine disease (43 for suspected APA, 3 for suspected CPA, and 1 for suspected pheochromocytoma). Nine suspected-NFA patients (16.1%) underwent adrenalectomy because of tumor growth. Three patients with suspected primary APA did not undergo surgery because of a poor physical condition. Five patients received medical treatment for suspected primary IHA.

The outcome assessment criteria for postoperative patients with adrenocortical lesions are listed in the supplemental materials (11). The outcomes for PA and Cushing syndrome patients were classified into 3 groups (cured, improved, or not improved), whereas the NFA patients were classified into 2 groups (not improved or not changed). The median follow-up time from surgery was 22.2 ± 3.9 mo. A flow diagram of patient enrollment, treatment, and follow-up evaluations is presented in Figure 1.
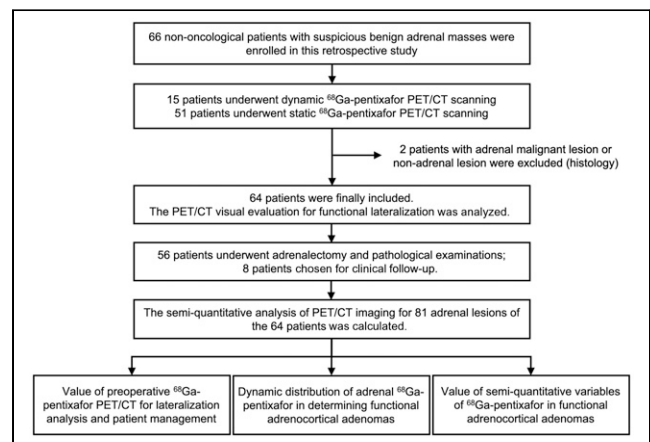

FIGURE 1. Flow diagram for enrollment, diagnosis, treatment, and follow-up examinations of patients.

TABLE 1
Baseline Characteristics of the 64 Patients

Characteristic	Data
Age (y)	47 ± 10
Sex	
Male	33
Female	31
BMI (kg/m^2)	25.3 ± 3.3
Hypertension (n)	53
Refractory hypertension (n)	20
Duration of symptoms (y)	7.4 ± 6.1
Systolic pressure (mm Hg)	175.0 ± 29.4
Diastolic pressure (mm Hg)	107.2 ± 16.7
Serum potassium (mmol/L)	2.9 ± 0.9
ARR ([ng/dL]/[ng/mL/h])	151.8 ± 66.7
Serum corticosteroid (μg/dL)	15.7 ± 5.8
ACTH (pg/mL)	20.2 (15.5–28.8)
24-h NE (μg/24 h)	25.4 ± 7.5
24-h UFC (μg/24 h)	79.9 (43.4–82.0)
Lesion location	
Right	24
Left	27
Bilateral	13

BMI = body mass index; ARR = aldosterone-renin ratio; ACTH = adrenocorticotropic hormone; NE = noradrenaline; UFC = urinary free cortisol.

Histology and Immunohistochemistry of CXCR4

Hematoxylin and eosin staining and immunohistochemical analyses were performed using paraffin-embedded specimens by 2 experienced pathologists. Hematoxylin and eosin staining was performed according to routine clinical protocols. Immunohistochemical analysis of CXCR4 was performed on 36 patients using paraffin-embedded specimens. The dilution of the CXCR4 antibody (ab124824; Abcam) was 1:100. For each tumor, a value designated as the H score was calculated by multiplying the intensity score and the positive percentage

score. Subsequently, the H score was classified into 3 groups (0–3, 4–8, and 9–12). Then, the differences in the SUV$_{max}$ of ^{68}Ga pentixafor among the 3 groups were calculated and analyzed. The analysis of the immunohistochemistry of CXCR4 is included in the supplemental materials.

Statistical Analysis

All data were processed using SPSS, version 22.0 (IBM), and Prism, version 8 (GraphPad), statistical software. The sensitivity and specificity of ^{68}Ga-pentixafor PET/CT visual analysis for adrenal functional lateralization were calculated. The semiquantitative variables (SUV$_{max}$, LLR, and LCR) were compared using ANOVA in categorized adrenocortical lesions (adenoma-active, adenoma-inactive/ hyperplastic). The Pearson correlation between the SUV$_{max}$ and the H score was calculated. The sensitivity and specificity of ^{68}Ga-pentixafor PET/CT semiquantitative analysis for discriminating the adenoma-active group from the non–adenoma-active group were calculated. Receiver-operating-characteristic curves were analyzed to calculate the thresholds of semiquantitative variables for the identification of active adrenal adenomas. Analysis items with a P value of less than 0.05 were considered statistically significant.

RESULTS

Baseline Characteristics and Clinical Management of Patients

Sixty-four patients (33 women and 31 men) aged 47 ± 10 y were included in our study. Their baseline clinical characteristics are listed in Table 1, and detailed information on all patients is listed in Supplemental Table 1. The final diagnoses of these 64 patients included 51 cases of PA (40 of APA, 3 of suspected UAH [details are in the supplemental materials (11)], and 8 of IAH), 3 of CPA, 8 of NFA, and 2 of pheochromocytoma (Table 2). Of the PA patients, 98% (50/51) had hypertension and 86.3% (44/51) had hypokalemia. Three CPA patients had typical cushingoid symptoms, including weight gain, facial plethora, menstrual disorder, increased waist circumference, and proximal muscle weakness. Six of the 8 NFA patients had no discernible symptoms, and 2 had essential hypertension. One pheochromocytoma patient presented with paroxysmal hypertension, and another was asymptomatic, with a silent pheochromocytoma lesion. Regarding the laboratory findings, PA patients showed higher plasma aldosterone-renin ratios than did the other groups (P < 0.05). Patients with CPA had increased serum corticosteroid levels and increased 24-h urinary free cortisol levels. Thirty-eight (74.5%) PA patients underwent

TABLE 2
Clinical Diagnosis, Treatments, and Results of ^{68}Ga-Pentixafor PET in the 64 Patients

Primary diagnosis	Treatments	Final diagnosis	^{68}Ga-pentixafor–positive
APA (46)	42 UA,1BA, 3 MT	40 (APA) + 3 (sUAH) + 3 (IAH)	39 (APA) + 3 (sUAH)
IAH (5)	5 MT	5 (IAH)	1 (IAH)
CPA (3)	2 UA,1 BA;	3 (CPA)	3 (CPA)
NFA (9)	9 UA	8 (NFA) + 1 (PCC)	1 (NFA)
PCC (1)	1 UA	1 (PCC)	0

UA = unilateral adrenalectomy; BA = bilateral adrenalectomy: MT = medicine therapy; sUAH = suspected UAH; PCC = pheochromocytoma.

Primary diagnosis was determined at baseline by endocrinologists and urologists from clinical and imaging presentations. Final diagnosis was determined after treatment according to diagnostic criteria listed in supplemental materials.

TABLE 3
Imaging Performance in the 64 Patients (81 Adrenal Lesions)

Lesion type	No. of lesions	Length on CT (cm)	SUV_{max}	LLR	LCR
APA	41	1.8 ± 0.7	15.3 ± 7.7	6.7 ± 4.5	5.6 ± 3.3
Suspected UAH	5	1.1 ± 0.4	9.1 ± 2.7	2.7 ± 0.7	2.1 ± 0.6
IAH	15	1.3 ± 0.5	4.3 ± 1.3	1.4 ± 0.5	1.7 ± 0.6
CPA	4	2.5 ± 0.7	21.9 ± 9.2	7.3 ± 2.3	14.9 ± 11.2
NFA	14	1.9 ± 0.8	4.4 ± 1.7	1.7 ± 0.7	1.7 ± 0.8
Pheochromocytoma	2	1.6; 4.7	1.7; 3.4	0.3; 1.0	1.7; 1.1

the captopril challenge test, which was positive in 35 (92.1%) (Supplemental Table 1).

Lesional Characteristics and Clinical Imaging Manifestations

There were 81 adrenal lesions (1.8 ± 0.8 cm; range, 0.6–4.0 cm) in these 64 patients, including APA ($n = 41$), suspected UAH ($n = 5$), IAH ($n = 15$), CPA ($n = 4$), NFA ($n = 14$), and pheochromocytoma ($n = 2$). All lesions presented with typical benign manifestations on CT imaging, with homogeneous and smooth margins (except for pheochromocytoma lesions presenting multiple cystic changes within the tumor). The imaging features of these lesions are shown in Table 3.

Visual Assessment by ^{68}Ga-Pentixafor PET Imaging and Outcome

In the visual per-patient analysis, 97.5% (39/40) of APA patients, 100% (3/3) of suspected-UAH patients, and 100% (3/3) of CPA patients had positive ^{68}Ga-pentixafor PET/CT results, whereas 87.5% (7/8) of IAH patients, 87.5% (7/8) of NFA patients, and 100% (2/2) of pheochromocytoma patients had negative results. These adrenocortical lesions were classified into either an APA/UAH/CPA group or an IAH/NFA group. The sensitivity and specificity of ^{68}Ga-pentixafor PET for functional lateralization (identification for APA, UAH, and CPA) were 97.8% (45/46) and 87.5% (14/16), respectively. Representative ^{68}Ga-pentixafor PET/CT images of patients with unilateral adrenal cortical nodules are shown in Figure 2.

In 51 PA patients, true positivity for ^{68}Ga-pentixafor adrenal uptake occurred in 42 patients (39 with APA and 3 with suspected UAH) (97.7%, 42/43), and true negativity for uptake occurred in 7 IAH patients (87.5%, 7/8). A false-negative result was found in 1 APA patient, and a false-positive result occurred in 1 IAH patient. Ten PA patients presented with bilateral adrenal lesions, and ^{68}Ga-pentixafor successfully identified the functional lateralization in 9 patients. A total of 37 APA patients underwent adrenalectomy (36 unilateral and 1 bilateral), resulting in cure in 24 patients and improvement in 13

patients. Three suspected-UAH patients underwent unilateral adrenalectomy and were cured, whereas 3 IAH patients underwent adrenalectomy because of a clinical misdiagnosis of APA; 2 of these patients showed no improvement, whereas 1 patient showed improvement.

All 3 Cushing syndrome patients showed ^{68}Ga-pentixafor–avid adrenal nodules (2 unilateral and 1 bilateral); all these patients were cured after adrenalectomy (2 unilateral and 1 bilateral).

Seven (87.5%) of the 8 NFA patients had a true-negative PET result; 1 NFA patient had a false-positive PET result. Eight NFA patients underwent a unilateral adrenalectomy. Two of these patients remained nonimproved, with 6 of these showing no change. The PET results of the 2 pheochromocytoma patients were both negative.
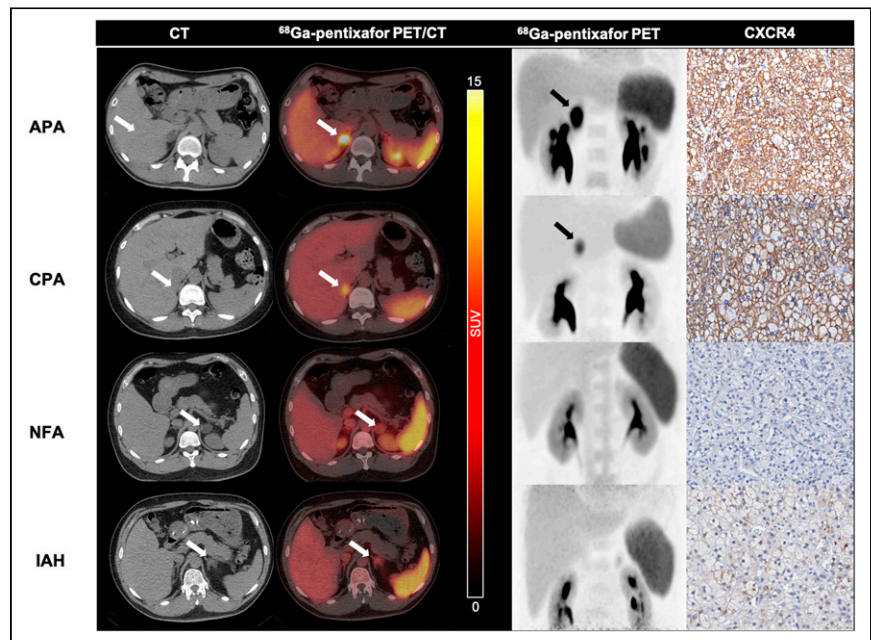

FIGURE 2. Performance of ^{68}Ga-pentixafor PET/CT imaging in patients with adrenal cortical nodules. (First row) Right adrenal APA (2.9 cm in long diameter on CT imaging, arrow) with positive findings on PET/CT and PET scanning (SUV_{max}, 29.0; arrows) and strong expression of CXCR4. Patient was 34-y-old man with 5-y history of hypertension and 0.5-y history of hypokalemia (serum potassium, 2.9 mmol/L). (Second row) Pentixafor-avid CPA in left adrenal gland (SUV_{max}, 14.8; 1.9 cm in diameter on CT, arrows) in 36-y-old woman with Cushing syndrome. Strong expression of CXCR4 was observed on immunochemical staining. (Third row) Non–pentixafor-avid NFA in left adrenal gland (SUV_{max}, 3.8; 2.9 cm in long diameter on CT imaging, arrows) in 36-y-old man. This adenoma had no increases in CXCR4 expression. (Fourth row) Negative IAH lesion (1.5 cm in long diameter on CT imaging, arrow) in 46-y-old man on ^{68}Ga-pentixafor PET/CT and PET imaging (SUV_{max}, 4.3; arrow). No increased expression of CXCR4 was observed by immunochemical staining.

Semiquantitative Analysis of PET/CT

The SUV_{max}, LLR, and LCR of the adrenocortical tumors are listed in Table 3. The highest radiotracer uptake was identified in patients with APA (SUV_{max}, 36.4). In addition, a significant correlation between uptake on ^{68}Ga-pentixafor and histologic CXCR4 expression was noted. The H score of CXCR4 correlated significantly with the SUV_{max} of ^{68}Ga-pentixafor ($r = 0.66$, $P < 0.0001$). The SUV_{max} of the 9–12 group for H score was significantly higher than that of the other 2 groups (Fig. 3). The uptake was significantly higher in the adenoma-active group than in either the adenoma-inactive group or the hyperplasia (suspected UAH and IAH) group (Fig. 3). The thresholds of SUV_{max}, LLR, and LCR and the corresponding sensitivities, specificities, and areas under the receiver-operating-characteristic curve to distinguish the adenoma-inactive group from the non–active-adenoma lesion group are shown in Figure 3.

Analysis of Dynamic PET Imaging

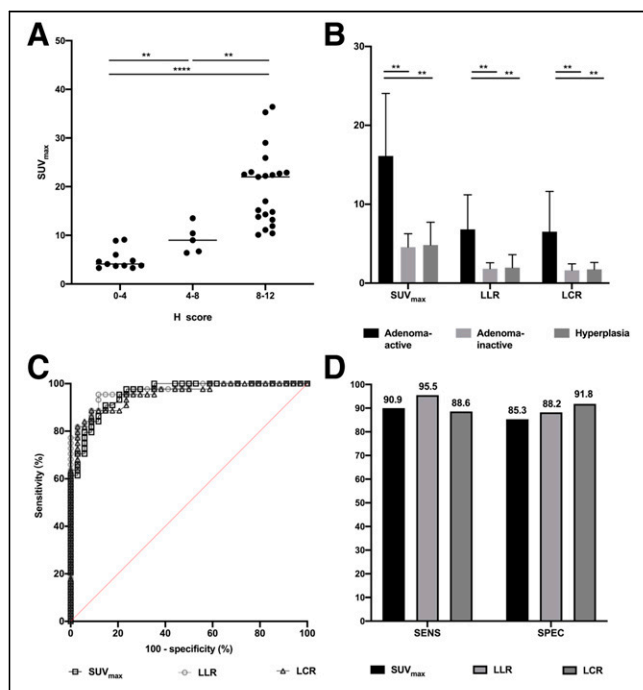The graphical influx rate constant was significantly higher for adrenocortical active adenomas (0.28 ± 0.8, $n = 11$) than for inactive adenomas (0.10 ± 0.06, $n = 5$, $P < 0.05$), normal adrenal glands (0.08 ± 0.04, $n = 16$, $P < 0.05$), or the liver (0.04 ± 0.03, $n = 16$, $P < 0.05$). Figure 4 shows the time–activity curves for normal adrenal tissue, liver, plasma, adrenocortical active adenomas, and inactive adenomas on ^{68}Ga-pentixafor dynamic PET/CT imaging in 15 patients. In this figure, the spots represent the mean SUV_{mean} at each time point, with the radioactivity distribution remaining stable after the early phase (5–10 min after injection).

^{68}Ga-Pentixafor Uptake and Outcomes

In the 48 patients with adrenocortical adenomas or hyperplasia who underwent adrenalectomy (except for 6 asymptomatic NFA patients), ^{68}Ga-pentixafor uptake in resected adrenal lesions was significantly higher in patients with preferable outcomes (cured and improved) than in those with nonpreferable outcomes (nonimproved) ($P < 0.001$, Fig. 5). The SUV_{max}, LLR, and LCR of ^{68}Ga-pentixafor in patients with preferable and nonpreferable outcomes were 15.5 ± 8.0 versus 4.2 ± 0.5, 6.5 ± 4.3 versus 1.3 ± 0.2, and 6.2 ± 5.0 versus 1.5 ± 0.6 ($P < 0.001$), respectively. Additionally, uptake was higher in the cured group than in the improved group but without statistical significance (Fig. 5).

Comparison Between AVS and ^{68}Ga-Pentixafor PET/CT

Four patients underwent both AVS and ^{68}Ga-pentixafor PET/ CT (Table 4). As determined by outcome evaluations, 2 patients with APA showed true-positive findings on both examinations, and 1 patient presented with a false-negative APA lesion on AVS versus a true-positive lesion on PET/CT. Additionally, 1 patient
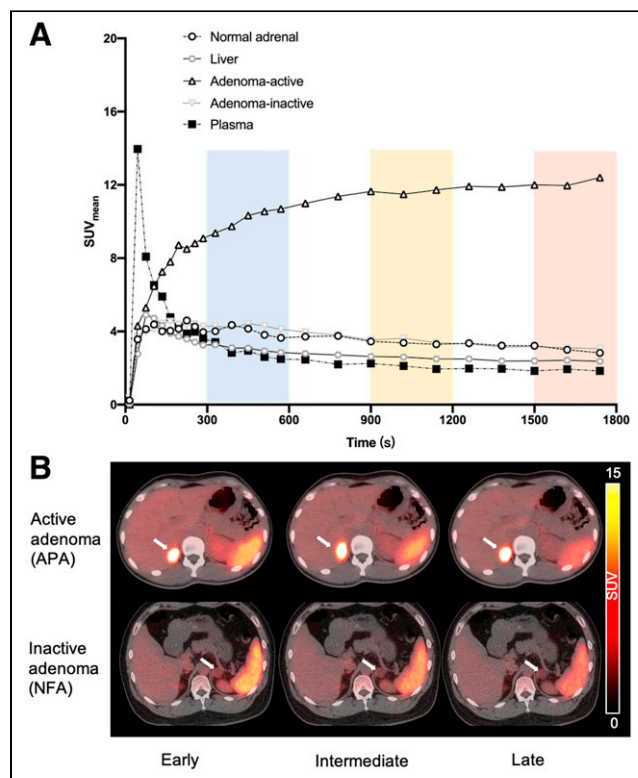

FIGURE 3. (A) ^{68}Ga-pentixafor SUV_{max} of 3 groups of H score (0–3, 4–8, and 9–12) were 5.0 ± 2.1 vs. 9.2 ± 2.9 vs. 19.8 ± 7.7, respectively. (B) ^{68}Ga-pentixafor SUV_{max}, ratio of lesional SUV_{max} to LLR, and ratio of lesional SUV_{max} to LCR for adenoma-active, adenoma-inactive, and hyperplastic lesions (SUV_{max}, 16.3 ± 7.9 vs. 4.4 ± 1.7 vs. 5.5 ± 2.7, respectively; LLR, 6.8 ± 4.3 vs. 1.7 ± 0.7 vs. 1.7 ± 0.8, respectively; LCR, 6.5 ± 5.1 vs. 1.7 ± 0.8 vs. 1.8 ± 0.6, respectively). SUV_{max}, LLR, and LCR were significantly higher for adenoma-active lesions than for adenoma-inactive or hyperplastic lesions. (C) Receiver-operating-characteristic analysis for determining optimal cutoffs for SUV_{max}, LLR, and LCR for differentiating active adenomas from non–active-adenoma lesions. Optimal cutoffs were 7.1, 2.5, and 2.4, respectively, with areas under receiver-operating-characteristic curve of 0.96, 0.97, and 0.95, respectively (all $P < 0.0001$). (D) Sensitivities and specificities of SUV_{max}, LLR, and LCR for identifying active adenomas. Sensitivities were 95.5%, 95.5%, and 84.1%, respectively, and specificities were 82.7%, 85.7%, and 91.4%, respectively.**$P < 0.001$. ****$P < 0.00001$.

FIGURE 4. (A) Time–activity curves for normal adrenal gland, liver, plasma, active adenomas, and inactive adenomas on ^{68}Ga-pentixafor dynamic PET/CT scans (30 min). Spots represent SUV_{mean} at each time point. (B) Representative ^{68}Ga-pentixafor PET/CT scans in patients with active adenoma and inactive adenoma at early (5–10 min), intermediate (15–20 min), and late (25–30 min) time points.
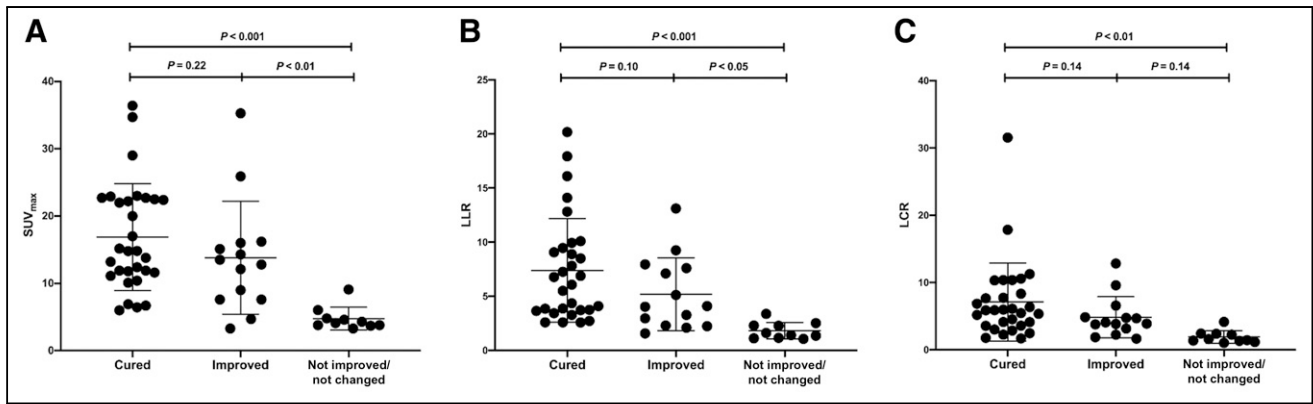
FIGURE 5. SUV$_{max}$ (A), ratio of lesional SUV$_{max}$ to normal LLR (B), and ratio of lesional SUV$_{max}$ to LCR (C) for ^{68}Ga-pentixafor in patients who were cured, improved, or not improved/not changed after adrenalectomy of adrenocortical lesions (SUV$_{max}$, 16.8 ± 8.1, 13.8 ± 8.4, and 4.8 ± 1.7, respectively; LLR, 7.4 ± 4.8, 5.2 ± 3.4, and 1.8 ± 0.8, respectively; LCR, 7.1 ± 5.0, 4.8 ± 3.1, and 1.9 ± 0.9, respectively).

with IAH presented with a false-positive result on AVS versus a true-negative result on PET/CT.

DISCUSSION

Functional lateralization in patients with adrenocortical lesions, along with discernment of functioning lesions from nonfunctioning lesions in nononcologic patients, is crucial for therapeutic management. Conventional lateralization and the functional assessment of adrenal masses are usually performed using adrenal CT or AVS. In this pilot study, we evaluated the performance of ^{68}Ga-pentixafor PET/CT for the functional lateralization of adrenal lesions and its effectiveness in identifying functional adrenal adenomas to help guide management decisions. The initial finding for APA lesion detection in patients with PA was reported in a pioneering study (*10*). In the present study, we further included 28 patients (22 with PA, 1 with NFA, 3 with Cushing syndrome, and 2 with pheochromocytoma) who had relatively heterogeneous adrenal tumor types, to extend the previous reports and provide complementary evidence of the potential for implementing screening for benign adrenal masses by ^{68}Ga-pentixafor PET/CT.

Diagnostic Efficacy and Clinical Significance of ^{68}Ga-Pentixafor PET/CT

Hormonal assessments are crucial when investigating adrenal masses; however, several important considerations must be accounted for during these evaluations, including daily hormonal rhythms, sex or age dependency, limitations of assays, substantial

variability in cutoffs, and drug interactions (*3*). In addition, it is important to remember that anatomic imaging approaches (e.g., CT imaging and MRI) are limited in their ability to functionally and molecularly characterize adrenal masses because of limitations in their resolution and specificity and the presence of substantial interobserver variation (*12*). In our study, ^{68}Ga-pentixafor PET was effective for the lateralization of adrenal disease. An APA patient with a single 0.6-cm lesion had a false-negative PET result in our study, which might indicate the limitation of this technique for small lesions with reduced spatial resolution. Semiquantitative variables (SUV and SUV ratios) yielded excellent sensitivities and specificities for discriminating active adrenocortical adenomas. The time–activity curves of the lesions showed a steady early tracer retention after tracer injection in active adenomas. ^{68}Ga-pentixafor PET/CT was negative for pheochromocytoma lesions, indicating the potential ability of ^{68}Ga-pentixafor to distinguish cortical from noncortical adrenal masses. Moreover, this study also demonstrated that ^{68}Ga-pentixafor has high sensitivity in the localization of CPAs. However, the number of cases was limited, and further prospective investigations are warranted to determine the values and pitfalls of ^{68}Ga-pentixafor in diagnosis and follow-up in patients with CPA.

In this study, patients who had a false-negative or false CT diagnosis could potentially be correctly diagnosed on the basis of the ^{68}Ga-pentixafor PET findings (supplemental results). However, further research is warranted regarding the utility of ^{68}Ga-pentixafor PET compared with CT for establishing a diagnosis and

TABLE 4
Comparison of AVS and ^{68}Ga-Pentixafor PET/CT Imaging Results

	AVS		^{68}Ga-pentixafor PET/CT				
Patient no.	Lateralization	Selectivity index	Lateralization	SUV$_{max}$	LLR	LCR	Clinical diagnosis
5	Right (index, 6.1)	30.8 (L); 13.2 (R)	Right	35.3	13.1	12.8	Right APA
34	Bilateral (index, 1.2)	5.4 (L); 3.5 (R)	Left	16.0	3.0	4.8	Left APA
39	Left (index, 62)	3.3 (L); 22.6 (R)	Left	7.6	2.2	3.2	Left APA
41	Left (index, 6.1)	54.8 (L); 31.5 (R)	Bilateral	4.3	1.6	2.4	IAH

Successful catheterization was defined as adrenal vein/peripheral vein cortisol ratio (selectivity index) of >3:1, and lateralization was defined as aldosterone/cortisol ratio (lateralization index) of >6:1 between left and right adrenal veins.

treatment plan in patients with adrenal disease. ^{68}Ga-pentixafor demonstrated a promising prognostic predictive value after therapy; nononcologic patients were more likely to have preferable outcomes after adrenalectomy for ^{68}Ga-pentixafor–avid adrenal lesions (Supplemental Fig. 1).

AVS is the gold standard for assessing the laterality of PA. AVS is technically challenging, with only a 50%–80% success rate for adrenal vein cannulation and a risk of complications (13–16). In our study, distinct results were identified between ^{68}Ga-pentixafor PET and AVS examinations. The consistency and difference between the 2 examinations need to be determined in further studies.

Potential Underlying Mechanisms for Adrenal Uptake of ^{68}Ga-Pentixafor

Published studies demonstrated that G protein–coupled receptors can increase the transcriptional and promoter activity of the *CYP11B2* (aldosterone synthase) gene, suggesting they may cause adenomas to increase their capacity to produce aldosterone (17,18). Previous studies have also shown that steroid production in some CPAs is regulated by aberrant expression of G protein–coupled receptors (19–21). However, Heinze et al. have demonstrated that only 26% of CPAs showed prominent CXCR4 expression (6). Further investigation is warranted to correlate ^{68}Ga-pentixafor uptake with CXCR4 expression.

Comparison to Other Radiopharmaceuticals

NP-59 has been used to investigate the secretory status of adrenal adenomas and to aid in lesion lateralization; however, this technique has significant shortcomings, including increased radiation exposure to the adrenal glands, longer acquisition procedures, low sensitivities, and poor spatial resolution (22). [123]I/^{11}C-metomidate, an inhibitor of 11β-hydroxylase, was introduced as a novel PET tracer for adrenocortical imaging; however, it could not distinguish between active and inactive adenomas (23). Moreover, the short half-life of ^{11}C limits its clinical use. In contrast, the acquisition time window for ^{68}Ga-pentixafor PET/CT imaging is long and be as early as 5–10 min after administration. All in all, ^{68}Ga-pentixafor PET/CT imaging may be a noninvasive, feasible, and effective method for preoperative diagnosis of adrenal incidentalomas, particularly for lateralization in patients with bilateral lesions.

Limitations

This study had several limitations. First, the fact that prospective randomization was not feasible at this stage potentially led to biases in selection and findings. Second, the statistical significance was not sufficient because of the small sample size. Thereby, a prospective, randomized, controlled trial is highly warranted to compare ^{68}Ga-pentixafor PET/CT with other approaches for obtaining preoperative diagnoses in patients with PA or suspected adrenal masses. Third, most of the positive findings in our study were APAs, as opposed to the small number of CPA cases, and there is a need to obtain further evidence of the capability of ^{68}Ga-pentixafor PET/CT in distinct types of functional adrenal masses.

CONCLUSION

[68]Ga-pentixafor exhibited excellent sensitivity and specificity for the functional lateralization of adrenal disease. ^{68}Ga-pentixafor PET/CT shows great potential for use in the therapeutic management of patients with adrenal masses.

KEY POINTS

QUESTION: Does ^{68}Ga-pentixafor have diagnostic and prognostic value for evaluating patients with primary adrenal cortical tumors?

PERTINENT FINDINGS: ^{68}Ga-pentixafor uptake was significantly higher in the adenoma-active group than in either the adenoma-inactive group or the hyperplasia group. Patients with ^{68}Ga-pentixafor–avid lesions had more preferable outcomes after adrenalectomy.

IMPLICATIONS FOR PATIENT CARE: ^{68}Ga-pentixafor showed excellent performance in the management of patients with typical benign adrenal lesions on CT imaging. This technique may also be a highly promising method for predicting patient prognosis after adrenalectomy.

REFERENCES

1. Mantero F, Terzolo M, Arnaldi G, et al. A survey on adrenal incidentaloma in Italy. Study Group on Adrenal Tumors of the Italian Society of Endocrinology. *J Clin Endocrinol Metab.* 2000;85:637–644.
2. Bourdeau I, El Ghorayeb N, Gagnon N, et al. Management of endocrine disease: differential diagnosis, investigation and therapy of bilateral adrenal incidentalomas. *Eur J Endocrinol.* 2018;179:R57–R67.
3. Funder JW, Carey RM, Mantero F, et al. The management of primary aldosteronism: case detection, diagnosis, and treatment: an Endocrine Society Clinical Practice Guideline. *J Clin Endocrinol Metab.* 2016;101:1889–1916.
4. Fassnacht M, Arlt W, Bancos I, et al. Management of adrenal incidentalomas: European Society of Endocrinology Clinical Practice Guideline in collaboration with the European Network for the Study of Adrenal Tumors. *Eur J Endocrinol.* 2016;175:G1–G34.
5. Garrett RW, Nepute JC, El Hayek M, Albert SG. Adrenal incidentalomas: clinical controversies and modified recommendations. *AJR.* 2016;206:1170–1178.
6. Heinze B, Fuss CT, Mulatero P, et al. Targeting CXCR4 (CXC chemokine receptor type 4) for molecular imaging of aldosterone-producing adenoma. *Hypertension.* 2018;71:317–325.
7. Kaemmerer D, Sänger J, Arsenic R, et al. Evaluation of somatostatin, CXCR4 chemokine and endothelin A receptor expression in a large set of paragangliomas. *Oncotarget.* 2017;8:89958–89969.
8. Williams TA, Lenders JWM, Mulatero P, et al. Outcomes after adrenalectomy for unilateral primary aldosteronism: an international consensus on outcome measures and analysis of remission rates in an international cohort. *Lancet Diabetes Endocrinol.* 2017;5:689–699.
9. Lacobone M, Citton M, Viel G, et al. Unilateral adrenal hyperplasia: a novel cause of surgically correctable primary hyperaldosteronism. *Surgery.* 2012;152:1248–1255.
10. Ding J, Zhang Y, Wen J, et al. Imaging CXCR4 expression in patients with suspected primary hyperaldosteronism. *Eur J Nucl Med Mol Imaging.* 2020;47:2656–2665.
11. Webb SM, Badia X, Barahona MJ, et al. Evaluation of health-related quality of life in patients with Cushing's syndrome with a new questionnaire. *Eur J Endocrinol.* 2008;158:623–630.
12. Kempers MJE, Lenders JWM, van Outheusden L, et al. Systematic review: diagnostic procedures to differentiate unilateral from bilateral adrenal abnormality in primary aldosteronism. *Ann Intern Med.* 2009;151:329–337.
13. Mulatero P, Bertello C, Sukor N, et al. Impact of different diagnostic criteria during adrenal vein sampling on reproducibility of subtype diagnosis in patients with primary aldosteronism. *Hypertension.* 2010;55:667–673.

14. Kline GA, So B, Dias VC, Harvey A, Pasieka JL. Catheterization during adrenal vein sampling for primary aldosteronism: failure to use (1-24) ACTH may increase apparent failure rate. *J Clin Hypertens (Greenwich).* 2013;15:480–484.

15. Seccia TM, Miotto D, De Toni R, et al. Adrenocorticotropic hormone stimulation-during adrenal vein sampling for identifying surgically curable subtypes of primary aldosteronism: comparison of 3 different protocols. *Hypertension.* 2009;53:761–766.

16. Lethielleux G, Amar L, Raynaud A, Plouin PF, Steichen O. Influence of diagnostic criteria on the interpretation of adrenal vein sampling. *Hypertension.* 2015;65:849–854.

17. Saner-Amigh K, Mayhew BA, Mantero F, et al. Elevated expression of luteinizing hormone receptor in aldosterone-producing adenomas. *J Clin Endocrinol Metab.* 2006;91:1136–1142.

18. Itcho K, Oki K, Kobuke K, et al. Aberrant G protein-receptor expression is associated with DNA methylation in aldosterone-producing adenoma. *Mol Cell Endocrinol.* 2018;461:100–104.

19. Dall'Asta C, Ballarè E, Mantovani G, et al. Assessing the presence of abnormal regulation of cortisol secretion by membrane hormone receptors: in vivo and in vitro studies in patients with functioning and non-functioning adrenal adenoma. *Horm Metab Res.* 2004;36:578–583.

20. Bugalho MJ, Li X, Rao CV, Soares J, Sobrinho LG. Presence of a Gs alpha mutation in an adrenal tumor expressing LH/hCG receptors and clinically associated with Cushing's syndrome. *Gynecol Endocrinol.* 2000;14:50–54.

21. El Ghorayeb N, Bourdeau I, Lacroix A. Multiple aberrant hormone receptors in Cushing's syndrome. *Eur J Endocrinol.* 2015;173:M45–M60.

22. Yen RF, Wu VC, Liu KL, et al. [131]I-6β-iodomethyl-19-norcholesterol SPECT/CT for primary aldosteronism patients with inconclusive adrenal venous sampling and CT results. *J Nucl Med.* 2009;50:1631–1637.

23. Minn H, Salonen A, Friberg J, et al. Imaging of adrenal incidentalomas with PET using ^{11}C-metomidate and ^{18}F-FDG. *J Nucl Med.* 2004;45:972–979.